Monte Carlo simulation study of the polymerization of polyurethane block copolymers: 4. Modelling of experimental data

Thomas A. Speckhard,* James G. Homan, John A. Miller* and Stuart L. Cooper†

Department of Chemical Engineering, University of Wisconsin, Madison, Wisconsin 53706, USA

(Received 5 March 1986; revised 16 June 1986)

Three different models that use the Monte Carlo method have been developed to predict the molecular weight, composition and hard-segment length distributions of polyurethane block copolymers polymerized under varying conditions. The simplest model tries to describe natural compositional heterogeneity that arises in polyurethanes due to the nature of the polymerization even under ideal conditions. The subsequent models introduce non-idealities into the simulation that actually occur in real polymerizations, including premature phase separation of the reactants and unequal reactivities of the monomer species. In this investigation, these models are used to simulate experimental data reported by MacKnight and coworkers on polybutadiene polyurethanes. The results of the modelling strongly support the hypothesis of MacKnight and coworkers that phase separation occurred near the beginning of the polymerization. The primary effect of the phase separation is to limit the degree of polymerization (molecular weight) in each phase presumably due to stoichiometric imbalances of reactants resulting from an unequal partitioning of the reactants in the two phases. The low molecular weights, in turn, lead to a broad composition distribution. The broad molecular weight distribution results from having a different average degree of polymerization in each phase, although allophanate crosslinking may also be a contributing factor. Differences between the three models and their utility for simulating experimental data are also discussed.

(Keywords: Monte Carlo simulation; polyurethane; block copolymers; polymerization; phase separation)

INTRODUCTION

Polyurethane block copolymers can be polymerized under a wide variety of conditions, leading to different molecular weight, hard-segment length and composition distributions[1-6]. The effects of changing these distributions on the morphology and properties of polyurethane block copolymers has generally received little attention although several studies have been reported describing the effects of varying one of the distributions[7-13]. Three major factors have inhibited progress towards gaining a better understanding of the effects of these distributions on sample properties and morphology. First, many investigators have ignored or neglected effects of this type without even attempting to gather experimental data for the distributions in their materials. It is likely that in many cases the effects due to varying these distributions are small especially in comparison to other varied parameters, yet without at least some experimental characterization, assuming the effects to be negligible may lead to erroneous conclusions concerning structure–property relationships. Secondly, it is difficult to obtain meaningful experimental data on the molecular weight, composition and hard-segment length distributions of polyurethane block copolymers. Information of this type is difficult to obtain for copolymers in general[14,15] and is even more difficult to obtain for polyurethanes because of their solubility characteristics, the many potential species that can be produced due to side reactions such as allophanate crosslinking, and also the fact that they are formed from three and not two different monomers[1,16]. This difficulty of characterization has no doubt fostered the neglect of effects of the type noted above. Finally, the complexity of the polyurethane polymerization reaction has hindered the development of a direct theoretical approach towards predicting the various distributions under given polymerization conditions. Peebles[5,6] has shown that under certain ideal conditions the hard-segment length distribution should follow a most probable distribution. Case[17] has derived equations describing the molecular weight distribution, but except for the calculation of $\bar{M}_n$ the equations are rather unwieldy. Lopez-Serrano *et al.*[18] have developed a method using a recursive technique that can be used to calculate averages of the various distributions.

One approach to overcoming some of the difficulties noted above is to use special synthetic techniques to produce simplified systems, for example, materials with approximately monodisperse hard-segment length distributions[12,13]. Materials of this type are valuable in two respects. First, since the hard-segment length is well defined, its effects on sample morphology and properties can be more directly elucidated. Secondly, the ability to

* Current address: 3M Research Center, St. Paul, MN 55144, USA.
† Author to whom correspondence should be addressed.

0032-3861/87/050768-09$03.00

control the hard-segment length distribution could be used to hold it constant while varying other parameters such as molecular weight.

An alternative approach is to develop models of the polymerization process that can be used to predict the composition, molecular weight and hard-segment length distributions of polyurethane block copolymers polymerized under various conditions. Models of this type are of interest because they can be used to simulate the effects of varying polymerization parameters on the various distributions. Also, it is possible by using models and a limited amount of experimental data to predict the entire composition, molecular weight and hard-segment length distributions. These calculated distributions could then be used along with experimental morphology and property data to investigate the effects of varying the distributions. The predicted distributions are, of course, only as good as the model and the assumptions therein and the quality of the experimental data. Furthermore, it is likely that many distributions can be simulated that produce the known experimental parameters. Obviously, the acquisition of more and better experimental data would allow for better distinction between various models, more accurate values of model parameters and/or increased model complexity.

In the first three contributions in this series[1-3], three different models were developed and described that use Monte Carlo methods to predict the molecular weight, composition and hard-segment length characteristics of polyurethane block copolymers polymerized under various conditions. The models differ in the assumptions made about the polymerization process, leading to the use of different parameters to describe various polymerization effects. Therefore, as discussed previously, a particular model may be more suited to describing a particular type of reaction, such as a one- or two-step polymerization[1-3]. Although the three different models (the single-phase ideal reaction model[1], the two-phase ideal reaction model[2] and the simple sinking pool model[3]) will be described briefly here, for more detailed information please refer to the original articles.

In the previous contributions[1-3] the effects of varying model parameters on the predicted distributions were investigated; however, actual experimental data were not modelled. The purposes of this investigation were (1) to demonstrate how the various models can be used to simulate experimental data, (2) to determine for a given material which model provides the 'best fit' and (3) to draw any conclusions or insights regarding the utility of the models and the structure–property relationships of the actual materials based on the results of (1) and (2). Therefore, in this contribution the three models described previously[1-3] will be used to simulate data on polybutadiene polyurethanes reported by MacKnight and coworkers[19,20]. These materials, which are described below, were chosen for study for several reasons. First, experimental molecular weight and composition information was already available[19-22]. Secondly, these materials were thought to have undergone phase separation during polymerization due to the incompatibility of the reactants, leading to unusual molecular weight and composition distributions, and thus were good candidates for modelling by the two-phase ideal reaction and simple sinking pool models. Finally, the results of the previous investigations by MacKnight and coworkers demonstrate the large effects on morphology and properties that can be associated with large changes in the composition, molecular weight and hard-segment length distributions. However, it should be noted that it was not the objective of this investigation to determine the effects of varying a particular distribution on the sample properties or morphology. The various models and the materials to be modelled are described briefly below.

DESCRIPTION OF MATERIALS

The synthesis and characterization of the polybutadiene-based polyurethane block copolymers has been reported by MacKnight and coworkers[19-22]. The samples were prepared using a two-step bulk reaction by reacting a hydroxy-terminated polybutadiene (PBD) oligomer ($\bar{F}_n = 1.97$, $\bar{M}_n = 2200$ and $\bar{M}_w/\bar{M}_n = 1.5$) with an isomeric blend of toluene diisocyanate (TDI) followed by chain extension with butanediol[23]. The product materials exhibited two hard-segment glass transition temperatures, low molecular weight and poor mechanical properties. Xu *et al.*[19] fractionated the samples into sol and gel fractions in *N,N*-dimethylformamide (DMF) at 70°C. They studied the composition and thermal characteristics of the resulting fractions by infra-red spectroscopy (i.r.) and differential scanning calorimetry (d.s.c.). The i.r. results indicated that the sol fraction had a much higher hard-segment content than the gel fraction. In effect, the sample could be thought of as a blend of two polyurethanes with different stoichiometries. For example, a blend of a material with a 10/9/1 molar ratio of isocyanate to chain extender to polyol with a 2/1/1 molar ratio material will produce a nominal 6/5/1 material with a bimodal hard-segment distribution and a broad composition distribution.

MacKnight and coworkers observed that when butanediol was added in the second step of the reaction it formed a separate phase immediately. This behaviour was observed for both crystallizable and non-crystallizable hard segments, indicating that the cause of the phase separation was not crystallization but the incompatibility of the reactants. A scenario for the polymerization was suggested where the isocyanate diffused into butanediol droplets and reacted to produce regions of virtually pure hard-segment polymer. The isocyanate-capped soft segments could not readily diffuse into the butanediol droplets and thus reacted primarily at the boundary between the two phases or by diffusion of butanediol into the soft-segment-rich phase. The final morphology of the polymer was largely determined by this phase separation during polymerization. The d.s.c. results of Xu *et al.*[19] showed that the sol and gel fractions exhibited different hard-segment glass transition temperatures that corresponded to the two T_g values observed in the unfractionated material. These transitions were attributed to long hard segments in the hard-segment-rich phase and short hard segments in the soft-segment-rich phase, respectively.

Xu *et al.* attributed the poor mechanical properties of these materials to the brittle behaviour of the hard-segment-rich material and to low overall molecular weight caused by an imbalance in isocyanate and hydroxyl groups in the individual phases of the reaction mixture. Subsequent work on PBD polyurethanes

synthesized in solution to reduce reactant incompatibility effects[22] led to higher molecular weights and improved physical properties. No evidence for compositional heterogeneity was observed in these samples in that two hard-segment T_g values were not observed and it was noted that samples could not be fractionated in DMF[22]. Finally, Xu *et al.* suggested that reactant incompatibility effects leading to compositional heterogeneity should be common in polyurethanes, but were especially evident in this system because of the large polarity difference of the reactants.

MODEL DESCRIPTIONS

The first and simplest model is the so-called single-phase ideal reaction model (SPI)[1]. This model is based on the assumptions of Peebles[5,6], notably equal reactivity of chain extender and polyol and no effects of molecular weight (chain length) on reactivity, that lead to a most probable distribution of hard-segment lengths at 100% conversion. The other major assumption is that the block degree of polymerization (BD_p) (in terms of hard and soft segments) follows the most probable distribution. Also, the model assumes stoichiometric conditions. Prior to the building up of any chains, three large arrays representing the block degree of polymerization distribution, hard-segment length distribution and soft-segment length or molecular weight distribution are created based on the values of various selected parameters such as the stoichiometry, average $\overline{BD_p}$, etc. The soft-segment molecular weight distribution is based on experimental data or a Schultz distribution with a known $\bar{M}_w/\bar{M}_n$ value can be used. The Monte Carlo methodology is then implemented as follows. First, a BD_p is selected at random from the BD_p distribution arrays and a random assignment of either beginning with a hard or soft segment is made. Hard and soft segments are then alternately selected at random from the appropriate array and added to the growing chain until the selected BD_p value is reached. The process is then repeated for the next chain and is continued until typically 15000 chains have been created. The molecular weight, composition and hard-segment length distributions can then be calculated and a simulated fractionation into low and high hard-segment content fractions can be carried out. In the fractionation procedure, the weight fraction of chains starting with the lowest hard-segment content chains is summed up to a specified weight fraction. The fractionation thus takes place solely on the basis of composition. The average molecular weight and composition for that fraction and the remaining fraction are then calculated. These data can then be compared to experimental fractionation data of the type reported by Xu *et al.*[19]

The second model, the two-phase ideal reaction model (TPI)[2], is a modified version of the SPI. The difference is that before building up any chains the monomer species are partitioned into two separate phases, one rich in the polyol species and one rich in the chain extender species. The fraction of polyol in the polyol-rich phase along with the fraction of diisocyanate in the hard-segment-rich phase can be selected. The model then divides the chain extender so that the reaction mixture in each phase is stoichiometric. After the monomers are divided between the two phases, the average block degree of polymerization is chosen for each phase, since there is no reason to believe that the degree of polymerization of each phase will be identical[24]. The building up of chains in the two phases is then done in the same manner as described for the single-phase ideal reaction model. Finally, before the simulation of fractionation or calculation of the various distributions the products of the two phases are recombined.

The third model, the simple sinking pool model (SSP), is fundamentally different from the other two models. In the previous models the chains were built up sequentially by whole soft or hard segments from what amounted to an infinite pool. In this model, the pool, which consists of monomers and not segments (and thus D_p and not BD_p values are used), is finite and the chains are polymerized simultaneously so that the simulation more accurately reflects the actual polymerization conditions. The probability of a given species being the next to react is not constant, as it was in the single-phase ideal reaction model, but depends on the number of that type of monomer remaining in the pool. There are other advantages to this method. The hard-segment sequence length distribution is not calculated using the equations of Peebles[5,6]. Therefore, the effect of finite molecular weight on the hard-segment sequence length distribution can be examined. Finally, the model can treat cases with excess isocyanate (non-stoichiometric) but does not include any effects due to crosslinking.

The SSP also allows simulation of two other effects, premature phase separation occurring at various points in the reaction and unequal reactivity of the chain extender and the polyol. Phase separation during polymerization is simulated by allowing a growing chain to have a memory of which diol (chain extender or polyol) species have recently been added to the chain and having the next diol to react be influenced by the previously reacted diols. The concept behind this is that chains that have recently reacted with a large number of chain extenders are more likely to be near a chain-extender-rich phase than near a polyol-rich phase. They will therefore be more likely to react with a diisocyanate followed by another chain extender than with a diisocyanate followed by a polyol. In the model, the self-affinity factor (*SAF*) determines the magnitude of this self-affinity effect while a second parameter (*NSA*) determines the D_p value for a given chain at which self-affinity effects start to be calculated. The self-affinity factor can be considered as representing the magnitude of the incompatibility of the reactants.

Non-equal reactivity of the diol species is handled in a similar fashion. The probability of reacting with a chain extender is multiplied by the reaction competitiveness factor (*RCF*) which can be greater or less than unity depending on whether the chain extender is thought to be more or less reactive than the polyol. Both the self-affinity and unequal reactivity effects can cause depletion of one of the monomers; however, at that point the probability of reacting with the depleted monomer type goes to zero since, as noted above, the probability of reaction also depends on the number of monomers in the pool.

The three models were designed for different polymerization conditions and purposes. The single-phase ideal model was designed to simulate one- or two-step solution polymerizations where the assumptions made by Peebles are most likely to be valid. Also, as shown in the next section, the model is useful as a test to determine whether non-ideal effects have occurred. The

two non-ideal models (TPI and SSP) are both designed to simulate phase separation during polymerization but have some noticeable differences. The two-phase ideal reaction model should be best suited for systems where phase separation occurs very early in the reaction while the sinking pool method can simulate phase separation at various points by changing the value of the *NSA* parameter. Also as noted above the degrees of polymerization are defined differently, with the result that the sinking pool method should be more accurate at very low degrees of polymerization. Additionally the sinking pool model allows for unequal reactivities of the chain extender and polyol but unlike the TPI model does not incorporate the diisocyanate reactivity ratio (μ) and is thus better suited for one-step reactions. Other differences between the models will become apparent in the next section.

RESULTS AND DISCUSSION

Table 1 contains a summary of the experimental composition and molecular weight data for the polybutadiene polyurethane samples reported previously[19,21]. The first column in *Table 1* identifies the sample with the nomenclature used by MacKnight and coworkers. The first part of the nomenclature (4T4, 4T10 or 6T4) identifies whether the sample is based on 2,4 (4T) or 2,6 (6T) TDI while the following 4 or 10 represents the approximate molar ratio of the isocyanate to the polybutadiene polyol. The middle part of the nomenclature, for example 4.2/3/1, is the ratio of the isocyanate to the chain extender (butanediol) to the PBD polyol used in the synthesis. The final number, for example 31.3, is the calculated hard-segment content (isocyanate plus chain extender) based on the amounts added in the synthesis and a $\bar{M}_n$ for the PBD soft segments of 2200 ($\bar{M}_w/\bar{M}_n = 1.5$).

The second and third columns in *Table 1* contain the weight fraction values for the portions of the sample that were found to be soluble or insoluble in DMF at 70°C[19]. The compositions of the soluble and insoluble fractions as determined by infra-red spectroscopy (i.r.) are listed in columns 4 and 5 and the overall compositions calculated from these data and the weight fraction values (columns 2 and 3) are listed in column 6. These values agree reasonably well with the values calculated based on the synthesis. Columns 7–11 contain composition data based on differential scanning calorimetry (d.s.c.) measurements. As noted previously, these materials exhibited two hard-segment T_g values that were ascribed to the hard- (phase 1) and soft- (phase 2) segment-rich phases respectively. The weight fraction and composition values for these phases were determined from the positions and magnitude of the glass transitions. The composition and weight fraction values determined by the i.r. and d.s.c. methods are in agreement for sample 4T10 but exhibit some discrepancies for the other two samples. For both samples 4T4 and 6T4 the i.r. fractionation data indicate a more even proportion of the hard- and soft-segment rich material. This behaviour would be expected to be accompanied by a decrease in the hard-segment content of the soluble fraction, as is observed, and an increase in the hard-segment content of the insoluble material, which is not observed. For both samples 4T4 and 6T4 the insoluble and phase 2 portions of the material have the same composition (17 and 15% hard segment respectively) but different weight fraction values. Thus for sample 4T4 the i.r. data indicate that 44% of the sample has an average weight fraction of 17% hard-segment content while the d.s.c. data indicate that 62% of the sample has an average weight fraction of 17%.

Careful consideration reveals that this result is only possible (assuming the data are accurate) if the lowest hard-segment content species in the sample are not included in the insoluble portion of the sample following the fractionation in DMF. This would not be unexpected since unreacted, low molecular weight, soft-segment polyol is likely to be soluble under the fractionation conditions. Thus, the fractionation takes place on some combined basis of composition and molecular weight. If fractionation took place solely on the basis of composition, the compositions of the soluble and insoluble portions would give rise to at least as broad a distribution as the phase composition based on the d.s.c. measurements. This fact is important for modelling considerations because all of the models assume that fractionation takes place solely on the basis of composition.

The final three columns in *Table 1* provide $\bar{M}_w$, $\bar{M}_n$ and $\bar{M}_w/\bar{M}_n$ values for the three samples based on gel permeation chromatography (g.p.c.) data and a *co*-(poly(ethylene oxide)–poly(ethylene glycol)) calibration curve[20]. Thus, these values are only relative and it is not even clear whether the true values are generally lower or higher than the values shown in *Table 1*[16,25]. Obtaining more accurate molecular weight values is difficult[25], and the relative nature of the measurement should not appreciably affect the $\bar{M}_w/\bar{M}_n$ values. The large $\bar{M}_w/\bar{M}_n$ values do clearly indicate the presence of non-ideal effects since under ideal conditions $\bar{M}_w/\bar{M}_n \leq 2$[1].

Table 2 contains the results of simulations performed using the single-phase ideal reaction model. In these simulations all of the model parameters were fixed except for the average block degree of polymerization ($\overline{BD}_p$). The value of A, the moles of isocyanate, was determined by the average composition. Note that the value of A does not correspond to the synthesis value (*Table 1*) because non-stoichiometric conditions cannot be modelled with the SPI and because the 'target' average composition value was taken as the value calculated from the fractionation

Table 1 Composition and molecular weight data for polybutadiene polyurethanes

	Weight fraction		Hard-segment content			Weight fraction		Hard-segment content					
Sample	Sol.	Insol.	Sol.	Insol.	Calc.	Phase 1	Phase 2	Phase 1	Phase 2	Calc.	$\bar{M}_w$	$\bar{M}_n$	$\bar{M}_w/\bar{M}_n$
4T4–4.2/3/1 – 31.3	0.56	0.44	41.7	17.0	30.8	0.38	0.62	53.0	17.0	30.7	28 800	7 300	3.9
4T10–10.5/9/1 – 54.5	0.80	0.20	67.5	10.5	56.1	0.80	0.20	67.5	10.5	56.1	32 300	4 400	7.3
6T4–4.2/3/1 – 31.3	0.54	0.46	35.0	15.0	25.8	0.38	0.62	43.0	15.0	25.6	18 300	3 000	6.1

Table 2 Results of simulations using the single-phase ideal reaction model

			Composition			Molecular weights						
						Overall			Insol.		Sol.	
Sample	$\overline{BD}_p$	A	Avg.	Insol.	Sol.	$\bar{M}_n$	$\bar{M}_w$	$\bar{M}_w/\bar{M}_n$	$\bar{M}_n$	$\bar{M}_w$	$\bar{M}_n$	$\bar{M}_w$
4T4-C	4.0	4.0	30.8	17.0	41.7	6200	11600	1.9	6400	11300	6000	12000
4T4-M_n	4.75	4.0	30.7	18.5	40.3	7400	13900	1.9	7500	13400	7200	14300
4T4-M_w	9.7	4.0	30.7	22.6	37.2	14900	28800	1.9	14800	27900	14900	29600
4T10-C	2.15	10.9	56.2	11.1	67.5	5300	9700	1.8	3200	5600	6300	10800
4T10-M_n	1.8	10.9	55.9	5.9	68.6	4400	8150	1.8	2700	4400	5300	9100
4T10-M_w	6.9	10.9	56.0	34.2	61.4	16900	32700	1.9	10400	20600	20000	35700
6T4-C	4.5	3.2	25.7	14.9	34.9	6100	12500	1.9	6900	12000	6100	12500
6T4-M_n	2.1	3.2	25.7	7.3	41.4	3100	5600	1.8	3400	5600	2700	5500
6T4-M_w	6.7	3.2	25.7	17.3	32.9	9700	18800	1.9	10100	18100	9400	19300

data (*Table 1*, column 5) and not the synthesis value. The values for the diisocyanate reactivity ratio μ (not shown) were 12 and 6 for 2,4 TDI and 2,6 TDI respectively[5]. The soft-segment molecular weight distribution was modelled by a Schulz distribution with $\bar{M}_n = 2200$ and $\bar{M}_w/\bar{M}_n = 1.5$[2,3]. Since 'lop-off' effects[1] were not considered to be likely because the polymerization was done in bulk, the only variable parameter was $\overline{BD}_p$. As $\overline{BD}_p$ increased, the molecular weights increased while the composition distribution became less broad.

For each sample, the results of three different simulations are reported in *Table 2*. The sample designations, for example 4T4-C, 4T4-$\bar{M}_n$ and 4T4-$\bar{M}_w$, indicate whether the $\overline{BD}_p$ value was adjusted to match the experimental composition (from fractionation data), $\bar{M}_n$, or $\bar{M}_w$ data. The resulting composition distributions for sample 4T4, can be seen in *Figure* 1, which shows that the simulations exhibit similar but distinct composition distributions. (As discussed previously[1-3], *Figure 1* is a plot of the intermediate weight fraction *versus* composition. The x-axis is the cumulative weight fraction of chains summed in ascending order of hard-segment composition. As x increases, the chains within an x interval possess a higher average hard-segment content than chains in previous x intervals. The y-axis is a measure of this change and is termed the specific hard-segment weight fraction.) Obviously, the SPI model cannot even approximately match the composition and molecular weight values simultaneously. In particular, as noted previously the model cannot produce $\bar{M}_w/\bar{M}_n$ values greater than 2 and thus the experimental values $\bar{M}_w/\bar{M}_n \geq 4$ are a strong indication of non-ideal reaction conditions. This is an important point because the model can be used to simulate the composition data and the resulting molecular weight values, especially $\bar{M}_n$, are not that inadequate considering the inaccuracies in and the relative nature of the molecular weight measurements. It should also be noted that the composition data based on the d.s.c. measurements could serve as an alternative to the fractionation data as a basis for the composition modelling. This suggestion has merit in that, although the model simulates a fractionation procedure, it appears that the experimental fractionation occurred at least partly on the basis of molecular weight and the resulting values indicate a narrower composition distribution than would be expected if the fractionation, as the model assumes, occurred based solely on composition. Thus, the

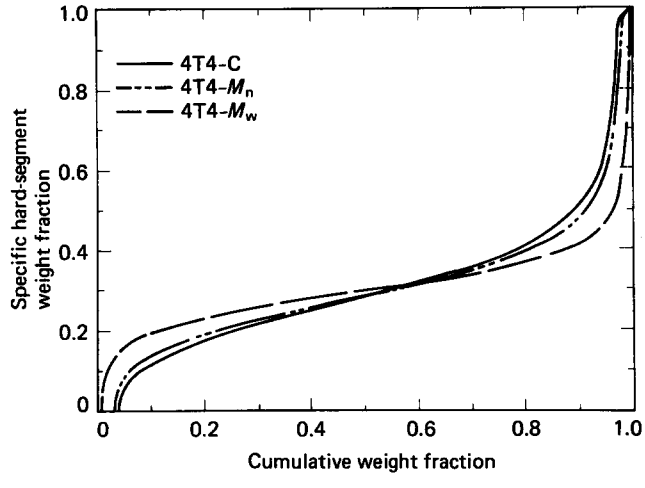

Figure 1 Specific hard-segment weight fraction *versus* cumulative weight fraction for the single-phase ideal reaction model samples 4T4-C, 4T4-M_n and 4T4-M_w

phase compositions, which in two cases indicate a broader composition distribution, might serve as better target values. Nevertheless, when these values were used as target values (data not shown) the resulting match of $\bar{M}_n$ and $\bar{M}_w$ was not significantly better than the results presented in *Table 2*. Finally, it is important to note that the composition-matched data do indicate that the primary effect of whatever non-ideality is occurring during the polymerization is to limit the molecular weight of the system. In other words, the observed broad composition distribution is not unexpected (or is primarily of 'natural' origin[1]) in light of the low molecular weight values.

The results of simulations performed using the two-phase ideal reaction model are displayed in *Table 3*. Since the TPI method contains additional parameters, namely the composition of the phases (the amount of methylene bis(*p*-phenyl isocyanate) (MDI) and PBD in the MDI- and PBD-rich phases respectively) and the $\overline{BD}_p$ of each phase, the modelling does not proceed in exactly the same fashion as for the SPI model. To begin with however, the values of μ, A and the soft-segment molecular weight parameters were fixed as described previously. At this point, two different approaches were used. If the d.s.c.-based 'phase' compositions were used as targets, the values of the fraction of MDI in the MDI-rich phase and

Table 3 Results of simulations using the two-phase ideal reaction model

Sample	A	$\overline{BD}_p1$	$\overline{BD}_p2$	Fractions[a] MDI	Fractions[a] PBD	Composition Phase 1	Composition Phase 2	Composition Avg.	Composition Insol.	Composition Sol.	Molecular weights Overall $\bar{M}_n$	Overall $\bar{M}_w$	Overall $\bar{M}_w/\bar{M}_n$	Insol. $\bar{M}_n$	Insol. $\bar{M}_w$	Sol. $\bar{M}_n$	Sol. $\bar{M}_w$
4T4-P	3.96	13.0	3.8	0.62	0.745	53.0	16.8	30.8	11.7	45.9	7300	28700	3.9	6400	10500	8200	43300
4T4-C1	3.96	13.0	3.8	0.56	0.62	40.2	22.9	30.7	16.8	41.7	8100	26200	3.2	6700	11300	9600	38200
4T4-C2	4.0	15.0	3.4	0.55	0.62	39.7	23.8	30.8	16.9	41.9	7500	28700	3.8	6200	10800	9000	43200
4T10-P	11.0	6.0	1.05	0.97	0.315	64.5	7.4	56.0	9.9	67.7	5900	31200	5.2	2700	62600	8300	37700
6T4-P	3.25	11.3	1.55	0.61	0.70	43.1	15.1	25.9	5.2	44.0	3100	19300	6.3	2900	4400	3100	33000

[a] Fraction of total MDI in MDI-rich phase (phase 1) and fraction of total PBD in PBD-rich phase (phase 2)

the fraction of PBD in the PBD-rich phase could be calculated since the model does not allow for non-stoichiometric conditions. This condition was termed phase-matched and is indicated by a -P in the sample designation. When this approach was used it was not possible to achieve matching fractionation composition data. As expected, based on the previous discussion, the simulated fractionation composition data always indicated a broader composition distribution than the experimental data. Alternatively, matched fractionation composition data (-C sample designation) could be achieved but the simulated phase composition values indicated a composition distribution that was too narrow.

Several other points should be made with regard to the modelling procedure using the TPI model. First of all for composition-matched samples, the effects of varying the MDI/PBD fractions and $\overline{BD}_p1$ and $\overline{BD}_p2$ on the molecular weight and composition data are not independent. Thus a trial-and-error procedure was used. Similarly for the phase-matched simulations, the mathcing of the $\bar{M}_n$ and $\bar{M}_w$ values involved a trial-and-error procedure with $\overline{BD}_p1$ and $\overline{BD}_p2$. Because the phase-matched simulations only involved two varying parameters ($\overline{BD}_p1$ and $\overline{BD}_p2$) and because of the problems involved with the relationship of the fractionation simulation and experimental data, the phase-matched approach was favoured and *Table 3* only includes composition-matched results for one sample (4T4) for comparison.

The most significant data in *Table 3* are the molecular weight values. By proper manipulation of $\overline{BD}_p1$ and $\overline{BD}_p2$ it was possible under either phase-matched or composition-matched conditions to achieve simultaneously good matching with the $\bar{M}_n$ and $\bar{M}_w$ values, at least for samples 4T4 and 6T4. For sample 4T10 the inability to produce matched molecular weight values is a result of the definition of the degree of polymerization in terms of segments and not monomers. This assumption is particularly bad in the case of sample 4T10 because the average hard segment contains 21 monomer units whereas for samples 4T4 and 6T4 the average hard segment contains only 7 or 8 monomers. Thus a very low $\overline{BD}_p$ is needed to obtain the experimental $\bar{M}_n$ value (note the $\overline{BD}_p2$ value of 1.05 for sample 4T10). In fact for all three samples the $\overline{BD}_p2$ values are low enough that the error involved in using segments instead of monomers is probably appreciable and even better results might be obtained if the model was modified.

Table 3 also contains $\bar{M}_w/\bar{M}_n$ values for the simulated sol and gel (insoluble) fractions. These values reveal that the soft-segment-rich fraction (insol.) has a lower molecular weight and narrower molecular weight distribution. The fact that $\bar{M}_w/\bar{M}_n$ for the soluble fraction is much greater than 2 is a clear indication that the simulated soluble and insoluble fractions do not correspond directly to the simulated hard- and soft-segment-rich phases (phase 1 and phase 2) even for sample 4T10. If they did $\bar{M}_w/\bar{M}_n \simeq 2$ since by definition of the model $\bar{M}_w/\bar{M}_n \simeq 2$ in each of the phases. A plausible scenario based on the data would be that almost all of the hard-segment-rich phase (phase 1) is included in the soluble fraction along with some very low molecular weight hard-segment-rich (probably single hard segments ($BP_p = 1$)) material from the soft-segment-rich phase.

The results of the modelling using the TPI model support several conclusions regarding the polymerization of the PBD polyurethanes. First, considering the experimental accuracy, the excellent agreement between the simulated and experimental composition and molecular weight values using the TPI model strongly supports the hypothesis of MacKnight and coworkers that phase separation occurred near the beginning of the reaction. The major effect of this phase separation process appears to be the limitation of the molecular weight especially in the soft-segment-rich phase (note the low values of $\overline{BD}_p2$). The low molecular weight would be expected due to stoichiometric imbalances in each phase following phase separation[24] and as noted previously would also lead to the observed broad composition distribution. The broad molecular weight distribution (high $\bar{M}_w/\bar{M}_n$) values arise from the large difference between $\overline{BD}_p1$ and $\overline{BD}_p2$, although allophanate crosslinking may also be a factor leading to large $\bar{M}_w/\bar{M}_n$ values[21]. Based on the polymerization scenario suggested by MacKnight and coworkers it appears that little butanediol diffused into the PBD-rich regions and thus the PBD-rich phase is primarily the low molecular weight product of the first (prepolymer) step of the reaction. The high molecular weight portions of the soluble fractions in *Table 3* could be considered to have been the results of reactions of long hard segments with prepolymer segments at the interface of the hard-segment-rich regions.

The final model that was used to simulate the experimental composition and molecular weight data of the polybutadiene polyurethanes was the simple sinking pool model. The results obtained with this model are

shown in *Table 4*. However, before discussing these results the modelling procedure will be briefly described. The molar excess of isocyanate to chain extender (A/B) (note all ratios are based on one mole of polyol) was kept constant at the synthesis value but the absolute values of A and B were again adjusted to match the average composition calculated from the fractionation data. The soft-segment molecular weight characteristics were the same as noted above and μ values were unnecessary. It was then possible to manipulate the $\bar{D}_p$, SAF and NSA or the $\bar{D}_p$ and RCF parameters to obtain good matches to the fractionation composition and $\bar{M}_n$ values. Alternatively, the composition and $\bar{M}_w$ values could be matched but it was not possible to match the $\bar{M}_n$ and $\bar{M}_w$ data simultaneously. Varying the SAF or RCF gave rise to similar effects as expected[3]. *Table 4* displays the results of three simulations each for samples 4T4 and 4T10. In the first simulation of each set (-$\bar{M}_n$1) self-affinity is not used and only RCF along with D_p was varied. The effects of varying the parameters are not independent but varying $\bar{D}_p$ mainly influences the molecular weight values while changing RCF primarily affects the composition data. In the second simulation of each set (-$\bar{M}_n$2), RCF is set at 1.0 (ideal value) and the self-affinity factor (SAF) is varied with $NSA = 10$ and $\bar{D}_p$ equal to the same value as the $\bar{M}_n$1 simulation. A third simulation (-$\bar{M}_n$3) was performed with $NSA = 1$. Both simulations gave rise to similar molecular weight and composition data but as expected as NSA decreases the value of SAF necessary to achieve given composition values also decreases.

Based on the results of the modelling with the TPI model one might expect similar or even better results to be obtained with the simple sinking pool model because of the advantages of this model noted previously. However, despite those advantages, the results of the simulations using the SSP model shown in *Table 4* indicate that the simulated data, primarily the $\bar{M}_w/\bar{M}_n$ values, do not match the experimental data. This inadequacy of the model is a result of the manner in which the phase separation process is modelled. Although the self-affinity concept is appealing in that it is more flexible than the partitioning method used in the TPI model it generally does not produce very broad (>3) $\bar{M}_w/\bar{M}_n$ values. This deficiency can be attributed to the attempt to model a two-phase system with a single pool of monomers. This deficiency could be overcome at least partially if the model allowed the D_p of a growing chain to vary with reaction conditions in a similar fashion to the probability of reacting with a given monomer. That is, if the growing end of a chain is more likely to react, the chain should tend to have a higher D_p. In fact, self-affinity and unequal reactivity effects should lead to deviations from a most probable D_p distribution; however, there is no simple method for calculating what the distribution should be[3,18]. It should be possible using a Monte Carlo method similar to that of Chaumont *et al.*[26] to let the D_p distribution in general, and the D_p of any chain, vary with reaction conditions by giving all species in the pool (i.e. monomer, dimers, etc.) the opportunity to react with all other species. Thus two growing chains could combine whereas in the present model a growing chain can only react with monomer. Higher $\bar{M}_w/\bar{M}_n$ values can be achieved with the SSP model if all of the chains are assumed to start polymerizing at the same instant because of the accentuated depletion effects[3], but $\bar{M}_w/\bar{M}_n$ values greater than 5 still are not normally obtained.

The effect of changing the way the degree of polymerization is defined can be noted in the $\bar{D}_p$ values for the simulations of sample 4T10 using the SPI and SSP models. With the SPI model, $\overline{BD}_p$ for sample 4T10 was normally lower than the $\overline{BD}_p$ values for the other samples, while in the SSP model the $\bar{D}_p$ values are higher. The effect can also be seen in the molecular weight data for the soluble and insoluble fractions. In the SPI and TPI models, the M_n and M_w values for the sol fractions were generally the same or higher than the values for the insoluble fraction. However, the situation is reversed for the SSP model because there are many more low molecular weight high hard-segment content species. In the SPI and TPI models only chains with a BD_p of 1 and possibly 3 would fall into that category while in the SSP model pure hard segments with D_p values of 1 to about 10 would qualify.

A comparison of the three models can be made for sample 4T4 using *Figures 2* and *3*. *Figure 2* is a plot of the composition distributions for sample 4T4 using the SPI model (4T4-C, *Table 2*), the TPI model (phase-matched 4T4-P and composition-matched 4T4-C2, *Table 3*) and the SSP model (4T4-$\bar{M}_n$2, *Table 4*). The various composition distributions are not that dissimilar, which is not surprising because all of the models provide the same fractionation composition data except the phase-matched TPI simulation, which shows the greatest deviation from the other curves. Note that the phase-matched TPI data, which as discussed previously are probably more accurate, exhibit a composition distribution with two

Table 4 Results of simulations using the simple sinking pool model

						Composition			Molecular weights						
									Overall			Insol.		Sol.	
Sample	A/B	$\bar{D}_p$	RCF	SAF	NSA	Avg.	Insol.	Sol.	$\bar{M}_n$	$\bar{M}_w$	$\bar{M}_w/\bar{M}_n$	$\bar{M}_n$	$\bar{M}_w$	$\bar{M}_n$	$\bar{M}_w$
4T4-$\bar{M}_n$1	4.08/2.88	19	1.72	0	–	30.8	17.3	41.5	7300	16800	2.3	11800	20200	5700	14100
4T4-$\bar{M}_n$2	4.07/2.87	19	1.0	0.21	10	30.6	17.1	41.3	7500	16100	2.1	11500	18600	5800	14200
4T4-$\bar{M}_n$3	4.07/2.87	19	1.0	0.11	1	30.7	17.4	41.3	7400	15400	2.1	11000	17300	5800	13850
4T10-$\bar{M}_n$1	11.1/9.6	20	6.0	0	–	56.0	11.0	67.5	4500	13300	3.0	15300	28800	3800	9400
4T10-$\bar{M}_n$2	11.1/9.6	20	1.0	100	10	56.0	10.7	67.5	4500	12300	2.7	13300	31000	3800	7500
4T10-$\bar{M}_n$3	11.1/9.6	20	1.0	4.2	1	55.9	10.4	67.5	4500	9500	2.1	8500	13300	4000	8600
6T4	3.35/2.25	6.8	1.0	0	–	25.8	38.5	11.6	3100	7500	2.4	5800	8800	2300	6300

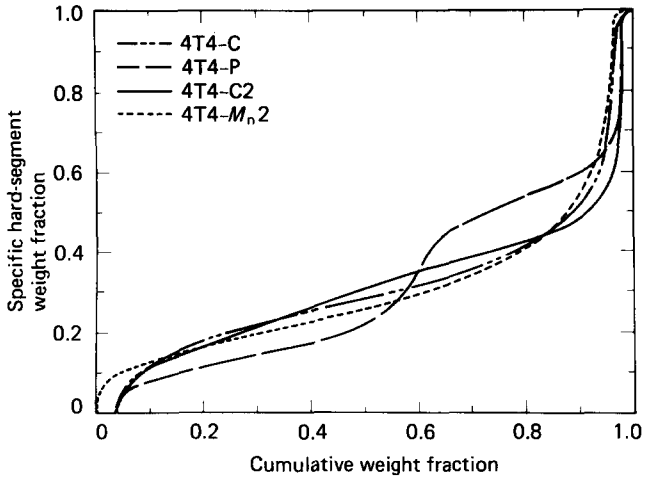

Figure 2 Specific hard-segment weight fraction *versus* cumulative weight fraction for samples 4T4-C (SPI), 4T4-P (TPI), 4T4-C2 (TPI) and 4T4-M_n2 (SSP)

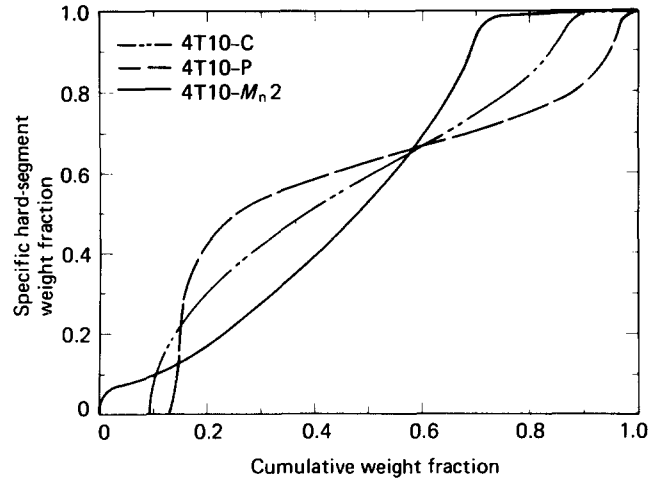

Figure 4 Specific hard-segment weight fraction *versus* cumulative weight fraction for samples 4T10-C (SPI), 4T10-P (TPI) and 4T10-M_n2 (SSP)

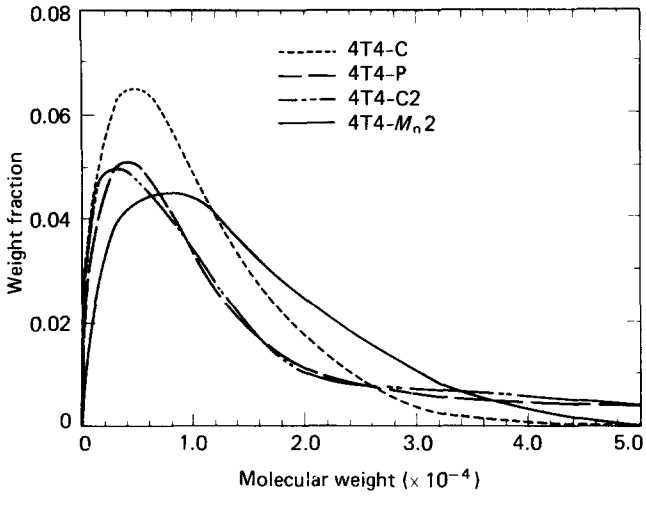

Figure 3 Molecular weight distributions for samples 4T4-C (SPI), 4T4-P (TPI), 4T4-C2 (TPI) and 4T4-M_n2 (SSP)

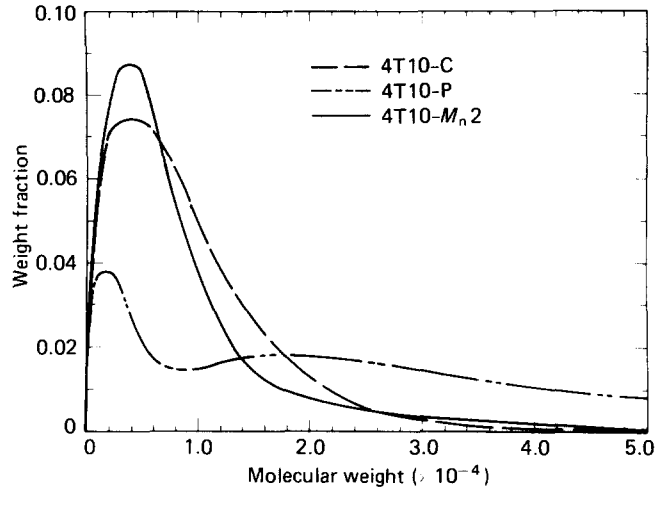

Figure 5 Molecular weight distributions for samples 4T10-C (SPI), 4T10-P (TPI) and 4T10-M_n2 (SSP)

plateaux characteristic of a material that underwent phase separation during polymerization. The molecular weight distributions (*Figure 3*) are markedly different and provide, as noted previously, a better basis for distinguishing between the three models. (As expected the distributions calculated using the TPI model are similar. However, these two simulated samples are easily distinguished on the basis of their composition distributions (*Figure 2*).) Similar conclusions can be drawn regarding sample 4T10 (*Figures 4* and *5*); however, the differences between the models are larger because of the greater effect of changing the way the degree of polymerization is defined and the broader experimental molecular weight ($\bar{M}_w/\bar{M}_n \sim 7$) and composition distributions of this sample.

SUMMARY AND CONCLUSIONS

Several conclusions can be drawn from the results of these attempts to model the experimental composition and molecular data of the polybutadiene polyurethanes previously studied by MacKnight and coworkers. First the fact that the data can be best simulated by the two-phase ideal reaction model supports the assertion made by MacKnight and coworkers that these samples underwent phase separation at an early stage in the polymerization. Furthermore, it appears that the major effect of the phase separation was to limit the molecular weight of the soft-segment-rich phase in particular, probably due to large stoichiometric imbalances of the reactants in the two phases. This low molecular weight in turn produced the expected and observed broad composition distribution. The phase separation process also led to a broad molecular weight distribution, which is probably due to the ability of the system to have different average degrees of polymerization in the two phases.

With regard to the models themselves, it is apparent that they have several shortcomings that could be improved for modelling actual experimental data. The fractionation procedure should be modified so that it could simulate molecular weight effects. The SPI and TPI models are not as accurate at low molecular weight because of the way they define the degree of polymerization, while the SSP model cannot give rise to large $\bar{M}_w/\bar{M}_n$ values. A superior model might be obtained by combining some of the features of the TPI and SSP models. Different modelling approaches that do not build up chains by adding monomers until a predetermined D_p

is achieved should be investigated. For example, a model that allows for any species in the pool (monomer, dimer, etc.) to react with any other species and with either functional group could be developed. This type of approach could also allow for the simulation of crosslinking, which is suspected to exist in the PBD polyurethanes[21] and may partially account for their broad $\bar{M}_w/\bar{M}_n$ values and solubility behaviour. For phase-separated systems the possibility of simulating diffusion by allowing the compositions of the phases to vary with time should be investigated. Numerous other improvements could also be made; however, most of the improvements increase the model complexity. More complex models in general require more experimental data to distinguish accurately between models or determine values of model parameters. For example, in the present study, the accuracy of the models could be further tested if molecular weight values for the soluble and insoluble fractions and/or data on the hard-segment length distributions were available. Obviously, additional experimental and theoretical work is needed to obtain a better understanding of the polyurethane polymerization process and a more accurate description of the resulting molecular weight, composition and hard-segment length distributions under various conditions.

ACKNOWLEDGEMENTS

The authors would like to acknowledge partial support of this research by the National Science Foundation, Division of Materials Research, Polymer Section, Grant No. DMR 86-03839 and through a grant from the Office of Naval Research. The authors would also like to thank Professor W. J. MacKnight for providing a copy of ref. 21 and Dr C. Feger for providing a copy of ref. 22 before publication.

REFERENCES

1 Speckhard, T. A., Miller, J. A. and Cooper, S. L. *Macromolecules* 1986, **19**, 1558
2 Miller, J. A., Speckhard, T. A. and Cooper, S. L. *Macromolecules* 1986, **19**, 1568
3 Miller, J. A., Speckhard, T. A., Homan, J. G. and Cooper, S. L. *Polymer* 1987, **28**, 758
4 Saunders, J. H. and Frisch, K. C. 'Polyurethane Chemistry and Technology: Part I, Chemistry', Interscience, New York, 1962
5 Peebles, L. H. *Macromolecules* 1974, **7**, 1872
6 Peebles, L. H. *Macromolecules* 1976, **9**, 58
7 Schollenberger, C. S. and Dinbergs, K. *J. Elastoplastics* 1973, **5**, 222
8 Schollenberger, C. S. and Dinbergs, K. *J. Elastoplastics* 1979, **11**, 58
9 Harrell, L. L. Jr *Macromolecules* 1969, **2**, 607
10 Ng, H. N., Allegrezza, A. E., Seymour, R. W. and Cooper, S. L. *Polymer* 1973, **14**, 255
11 Miller, J. A., Lin, S. B., Hwang, K. K. S., Wu, K. W., Gibson, P. E. and Cooper, S. L. *Macromolecules* 1985, **18**, 32
12 Eisenbach, C. D. *ACS Polym. Prepr.* 1985, **26**(2), 7
13 Qin, Z. Y., Macosko, C. W. and Wellinghoff, S. T. *ACS Polym. Mater. Sci. Eng. Prepr.* 1983, **49**, 475
14 Rempp, P. and Benoit, H. *Rubber Chem. Technol.* 1968, **41**, 245
15 Spatorico, A. L. *J. Appl. Polym. Sci.* 1974, **18**, 1793
16 Speckhard, T. A. Ph.D. Thesis, University of Wisconsin–Madison, 1985
17 Case, L. C. *J. Polym. Sci.* 1958, **29**, 455
18 Lopez-Serrano, F., Castro, J. M., Macosko, C. W. and Tirrell, M. *Polymer* 1980, **21**, 263
19 Xu, M., MacKnight, W. J., Chen, C. H. Y. and Thomas, E. L. *Polymer* 1983, **24**, 1327
20 Chen, C. H. Y., Briber, R. M., Thomas, E. L., Xu, M. and MacKnight, W. J. *Polymer* 1983, **24**, 1333
21 Chen-Tsai, C. H. Ph.D. Thesis, University of Massachusetts, 1985
22 Bengston, B., Feger, C. and MacKnight, W. J. *Polymer* 1985, **26**, 895
23 Brunette, C. M., Hsu, S. L., Rossman, M., MacKnight, W. J. and Schneider, N. *Polym. Eng. Sci.* 1981, **21**, 668
24 Tirrell, M., Lee, L. J. and Macosko, C. W. *ACS Polym. Symp.* 1978, **104**, 149
25 Lee, D. C., Speckhard, T. A., Sorenson, A. D. and Cooper, S. L. *Macromolecules* 1986, **19**, 2383
26 Chaumont, P., Gnanou, Y., Hild, G. and Rempp, P. *Makromol. Chem.* 1985, **186**, 2321